

Observation of Locked Optical Kink-Antikink Spatial Shock Waves

Barak Freedman,¹ Tal Carmon,¹ M. I. Carvalho,² Mordechai Segev,¹ and Demetrios N. Christodoulides³

¹*Department of Physics and Solid State Institute, Technion, Haifa 32000, Israel*

²*Department of Electrical Engineering and Computers, Oporto University, Porto, Portugal*

³*School of Optics/CREOL, University of Central Florida, Orlando, Florida 32816-2700, USA*

(Received 19 May 2003; published 23 September 2003)

We report the first experimental observation of optical spatial shock-wave pairs. The shock waves consist of two coupled kink and antikink beams that remain locked to each other throughout propagation in a nonlinear diffusion-driven photorefractive crystal. These coupled shock-wave pairs move undistorted at angles that fall outside their original angular sector of propagation.

DOI: 10.1103/PhysRevLett.91.133902

PACS numbers: 42.65.Sf

Shock waves have been thoroughly investigated in several branches of science including astrophysics, fluid mechanics, plasmas, and solid-state physics [1–3]. In optics, however, the observation of shock waves has thus far been very rare in spite of theoretical works suggesting their existence in various settings [4–17]. For example, spatiotemporal shocks (kinks) have been predicted in Raman systems [4–7], in dispersive amplifying Ginzburg-Landau systems that exhibit a frequency-dependent gain or loss [8,9], as well as in isotropic Kerr media [11,12] in the form of polarization kink states. In the spatial optical domain, shock waves have been suggested in quadratic bulk media and discrete waveguide arrays [13,14] as well as in photorefractive crystals [15,16]. From these examples it is clear that optical shock waves necessitate an energy-exchange process. Temporal shock waves can arise, e.g., during stimulated Raman scattering between a Stokes and a pump wave [5], intrapulse Raman scattering within a single shock-wave state [4,6,7] or a frequency-dependent amplification [8,9]. Similarly, spatial shock waves can exist as a consequence of an energy-exchange mechanism, such as that of two-wave mixing that occurs naturally in photorefractives [18,19]. In fact, kink-antikink shock-wave pairs have been predicted [15] in unbiased photorefractives, and a shock domain “soliton” has been suggested in biased photorefractive crystals exhibiting a drift nonlinearity [16].

Here we present the first experimental observation of optical spatial shock-wave pairs. These are two coupled kink and antikink beams, remaining locked to each other throughout propagation in a nonlinear diffusion-driven photorefractive crystal [15]. Our experiment demonstrates that these coupled shock-wave pairs move undistorted at angles that fall outside their original angular sector of propagation in a way analogous to their temporal counterparts that can exhibit superluminal/subluminal or tachyonic behavior [5]. The existence of this family of locked shock waves requires that energy is transferred from a strong “pump” (kink-shaped) beam to a weaker “signal” (antikink) beam. If in this same con-

figuration the situation is reversed, namely, if the pump is made weaker than the signal, the beams unlock and move away from one another, while becoming appreciably distorted.

We begin by recalling the theory of this class of shock-wave pairs [15]. Consider the evolution of two codirectional optical waves, henceforth referred to as beam *a* and beam *b*, propagating in the *xz* plane at angles $\pm\theta$ with respect to the *z* axis. The waves are shaped as two kinks facing one another (in the *x* direction), as shown schematically in Fig. 1 (left panel). The kinks are chosen to be fairly broad: the intensity changes from zero to its maximum value within a transverse distance of 100 μm (or more), so that diffraction effects can be neglected. In addition, the waves are uniform along *y*, hence their evolution depends only on the spatial variables *x* and *z*. The beams propagate in a photorefractive material which

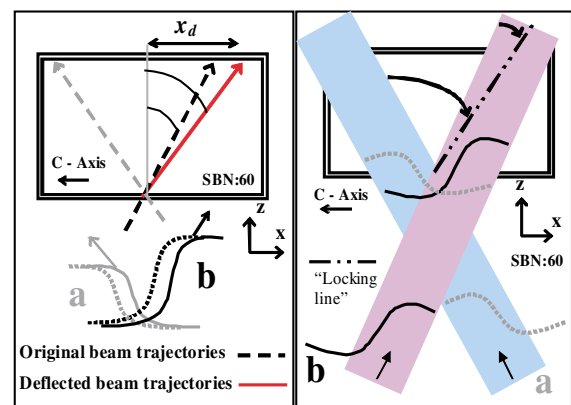


FIG. 1 (color online). Left: Schematics showing propagation of the two shock waves: the “signal” beam *a* and the “pump” beam *b*. θ is the original angle of incidence and φ the new angle of propagation of the locked shock wave pair. x_d is the lateral displacement of the “locking point” at the output plane of the crystal. Right: a top view schematic of the beams’ overlap at the input face of the crystal, and their lateral movement resulting in beam locking. The new propagation direction of the shock fronts is along the “locking line.”

is a dielectric crystal having impurities deep within the “forbidden gap.” Upon illumination, these dopants contribute free charge carriers, which redistribute and set up a space-charge field that depends on the structure of the optical intensity and modifies the refractive index through the electro-optic effect. In the absence of any external bias, these waves interact with each other via a diffusion-induced two-wave mixing process [15,18]:

$$\frac{\partial I_a}{\partial z} - v \frac{\partial I_a}{\partial x} - \gamma \frac{I_a I_b}{I_d + I_a + I_b} = 0, \quad (1a)$$

$$\frac{\partial I_b}{\partial z} + v \frac{\partial I_b}{\partial x} + \gamma \frac{I_a I_b}{I_d + I_a + I_b} = 0, \quad (1b)$$

where I_a and I_b are the intensities of the waves, $v = \tan(\theta)$ represents their transverse (spatial) “velocity,” I_d is the dark irradiance (a quantity proportional to the material’s dark conductivity), and γ is the two-wave mixing coupling coefficient [18,19]. Without any loss of generality, let us assume here that γ is positive, in which case power flows from I_b to I_a as a result of two-wave mixing amplification. In the absence of any two-wave mixing, the solutions of Eqs. (1) are given by $I_a = I_{a0}(x + vz)$ and $I_b = I_{b0}(x - vz)$ that indicate that the input intensity profiles remain invariant during propagation while moving along their initial trajectories $\pm v$. The angles $\pm\theta$ corresponding to these trajectories define the original “allowed” angular sector of propagation for these two wave fronts. If two-wave mixing is present, Eqs. (1) can exhibit kink-antikink shock-wave solutions [15]. To identify these solutions we assume that both waves move locked with each other along a characteristic coordinate $\xi = x - V_e z$, i.e., at a common velocity V_e . In this case the new angle of propagation associated with this dimensionless transverse velocity V_e is given by $\varphi = \tan^{-1}(V_e)$. Let the intensities of the two beams be expressed as

$$I_a(\xi) = rI_d X(\xi), \quad (2a)$$

$$I_b(\xi) = sI_d Y(\xi), \quad (2b)$$

where $X(\xi)$ and $Y(\xi)$ are normalized real functions (bounded between 0 and 1) describing the intensity profiles of the two beams, and the positive numbers s and r stand for the maximum intensity ratio of each beam with respect to I_d . Substituting Eqs. (2) into Eqs. (1) one obtains a new set of equations for $X(\xi)$ and $Y(\xi)$, having shock-wave solutions,

$$\left(\frac{v + V_e}{s}\right) \frac{dX}{d\xi} + \gamma \frac{XY}{1 + rX + sY} = 0, \quad (3a)$$

$$\left(\frac{v - V_e}{r}\right) \frac{dY}{d\xi} + \gamma \frac{XY}{1 + rX + sY} = 0. \quad (3b)$$

These shock waves $X(\xi)$ and $Y(\xi)$ propagate in the photo-refractive crystal *locked to one another*, without any change of form (distortionless), at a common transverse velocity

$$V_e = \left(\frac{s + r}{s - r}\right)v. \quad (4)$$

Figure 2(a) shows the results of a numerical simulation regarding the propagation of such shock waves when moving locked together. In this configuration, the energy transfer from the stronger beam I_b to the weaker beam I_a maintains the “shock structure” of the two beams, while transversely displacing them in a way that keeps the beams locked together. Had the medium of propagation been linear, that is, in the absence of any energy transfer process, the beams would have continued along their original trajectories, resulting in the separation of the kink and antikink beams (Fig. 1, right panel). Under the two-wave-mixing process, beam I_b is slightly displaced whereas beam I_a is displaced considerably more (Fig. 1), so their shock fronts lock together during propagation. The inset in Fig. 2(a) shows the magnified intersection region of the shock fronts. Figure 2(b) depicts the intensity profiles of these two beams at the output face of the crystal, with and without nonlinearity, displaying locked shock-wave propagation (solid) versus linear unlocked propagation (dotted).

We emphasize that locked shock-wave solutions of these equations exist *only if* the energy flows from the more intense beam to the weaker beam. This effect can be seen by comparing the simulation results of Fig. 2(a) to those of Fig. 2(c), the former with $I_a < I_b$, and the latter with $I_a > I_b$, and all other parameters remaining identical. Figure 2(a) shows locked shock-wave propagation, whereas in Fig. 2(c) the shock waves do not lock, but rather separate away from one another. These distinctly

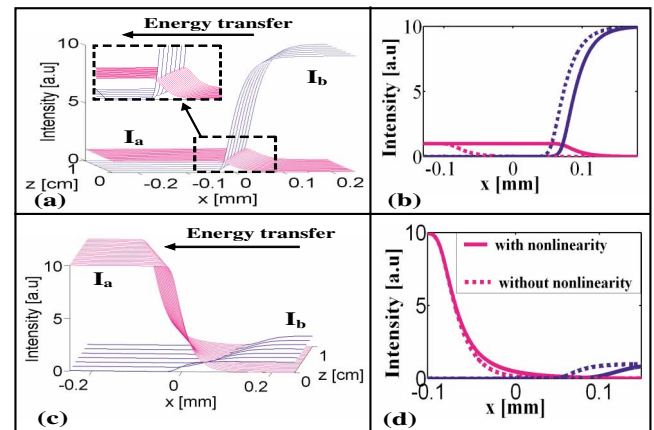


FIG. 2 (color online). Numerical simulations showing the propagation of the shock-waves pair through a 10 mm long nonlinear crystal. (a) Nonlinearity “on” and $I_b > I_a$: the shock waves lock and move together to the right, as also reflected in their output beam profiles shown in (b) with nonlinearity “on” (solid). Nonlinearity “off”: the beams separate, no overlapping at the output face of the crystal (dotted). (c),(d) Nonlinearity “on” but $I_b < I_a$: the shock waves do not lock, but rather further increase their separation (compared to linear propagation).

different behaviors are very clear while observing the output beam profiles in the two cases [Figs. 2(b) and 2(d)]. If energy flows from the weak beam to the strong one, the shock-wave form is distorted, and the “locking” is disabled. Each beam then continues in its original trajectory, and a gap forms between the beams at the crystal output plane [Figs. 2(c) and 2(d)]. We note that the sign of γ (the coupling coefficient) is determined by the polarity of the space-charge field with respect to the crystalline axes. It does not pose any experimental limitation: had γ been negative, we would set $I_a > I_b$.

Another interesting feature associated with the propagation of these locked shock waves has to do with their apparent “velocity.” The lateral displacement of the “locking point” of the two shock-wave beams at the output plane of the crystal is given by $x_d = V_e L$ where L is the length of the crystal and $V_e = \tan(\varphi)$, φ being the direction of propagation of the locked shock waves (Fig. 1). As pointed out in [15], Eq. (4) always requires that $\varphi > \theta$ and therefore the two locked shocks *move outside their original sector of propagation* $\pm\theta$ in a way analogous to their temporal counterparts that can exhibit superluminal/subluminal or tachyonic behavior [5]. What makes this behavior possible is the way the exponential tails of these shocks interact. The tails prepare the way for this self-similar exchange to occur and as a result the two waves move together at a higher velocity V_e . However, for this same reason, the shock shift cannot occur indefinitely. The tail of beam a (to be amplified) will eventually reach the noise floor and the pair will eventually disintegrate due to noise. This spatial effect is analogous to the quantum noise limits imposed on superluminal propagation [20].

Experimentally, we use a standard two-wave mixing setup, with a 114 mW DPSS Laser and a custom designed “mask” to generate the kink beams. The mask was fabricated by depositing nickel on a glass plate, thus achieving the desired kink pattern. The transparency profile for the mask goes from 0% to 100% within 300 μm distance. The 532 nm extraordinarily polarized beams are launched into a 7 mm long photorefractive SBN:60 crystal, having a refractive index of $n_e = 2.3$. The diffusion-driven two-wave-mixing process occurs naturally, without any bias field. We examine the propagation dynamics of these beams with and without the nonlinearity, so that we can draw a direct comparison between the locked state and the linear propagation (and separation) of the shock fronts. Experimentally, we distinguish between linear and nonlinear propagation by taking advantage of the nonzero response time of the photorefractive nonlinearity. Thus, monitoring the output beams at times much shorter (~ 10 m sec) than the photorefractive response time (~ 1 sec) gives the linear propagation results (nonlinearity “off”), whereas monitoring the beams after temporal steady state has been reached (~ 1 min) provides the nonlinear propagation results (nonlinearity “on”). The primary effect under study is

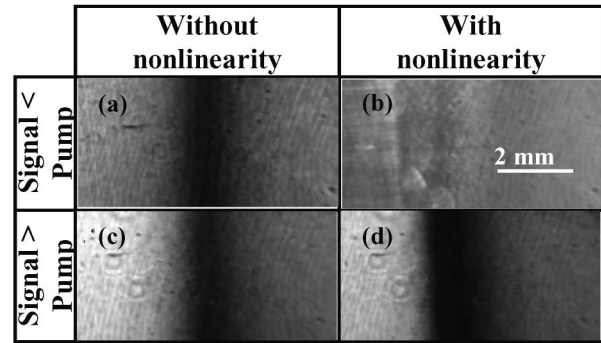


FIG. 3. Photographs of both beams at the output face of the crystal, displaying (a),(c) separated shock fronts during linear propagation, (b) locked shock waves when the signal is weaker than the pump ($I_b > I_a$), and (d) increased separation when the signal is stronger than the pump ($I_b < I_a$).

the locking mechanism of the two optical shock-wave beams. Typical experimental results are shown in Figs. 3 and 4, depicting photographs of the intensity structure of both output beams, for $I_a < I_b$ ($\sim 1:10$) and for $I_a > I_b$ ($\sim 10:1$). When the nonlinearity is “off,” the two input beams that overlap in their evanescent tails (at $z = 0$), follow their input trajectories and separate from one another, as depicted in Figs. 3(a) and 3(c). This is a consequence of linear propagation, so (obviously) it happens irrespective of the beam intensities. [Experimentally, Figs. 3(a) and 3(c) are taken at $t = 0$, before the photorefractive space-charge field builds up]. When the nonlinearity is on and reaches steady state, the beams behave in a very different fashion. For $I_a < I_b$ with the nonlinearity in steady state, the shock-wave beams lock to one another, and their shock fronts remain in contact at the crystal output face just as they overlap at the input face, as shown in Fig. 3(b). Since the beams’ tails overlap, the intensity gap between them is almost unnoticeable in the photograph of Fig. 3(b), depicting the total intensity (of both beams) at the output plane. To observe each individual beam while they are locked, we block one beam prior to the input plane and monitor the remaining beam at the output plane, within a time window

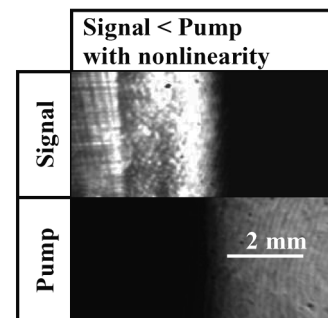


FIG. 4. Photographs of each of the locked beams of Fig. 3(b) monitored separately. The overlap between the beams remains unchanged throughout propagation.

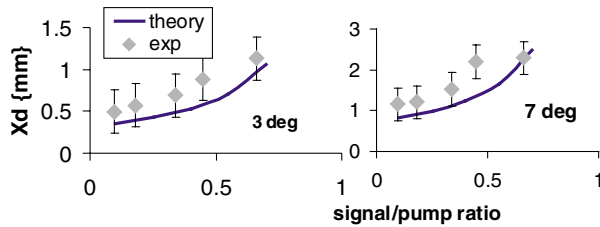


FIG. 5 (color online). Lateral displacement of the locked signal (shock-wave) beam at the output face of the crystal. The angle of incidence in air is 3° and 7° and the crystal length is 7 mm.

(~ 10 msec) much shorter than the response time of our nonlinearity (~ 1 sec). Figure 4 shows each beam separately, in a locked state [Fig. 3(b)]—the overlap between the beams remains unchanged throughout propagation. It is instructive to observe what happens when the intensities of the input beams are modified so that $I_a > I_b$, under the same parameters and with the nonlinearity in steady state. As predicted, for $I_a > I_b$ the beams do not lock but instead the separation between the beams increases [Fig. 3(d)] compared to their separation during linear propagation [Fig. 3(c)].

Another effect measured in the experiment is the lateral displacement of the beams at the output plane of the crystal. We measure the lateral displacement of the locked shock waves (with the nonlinearity on), by comparing the location of the output shock front in a locked state to the output during linear propagation. Figure 5 shows the lateral displacement of the shock front of the output signal beam as a function of signal/pump intensity ratio for various angles of incidence θ , along with the theoretically calculated displacement (solid curve). The displacement is equal to x_d plus the (off-center) displacement due to linear propagation. For example, when the angle of incidence (in air) is $\theta = 5^\circ$ and the intensity ratio is $r/s = 0.5$, the shock pair has propagated in a locked fashion and their locking point (shock front, dash-dotted line in Fig. 1, right panel) has been displaced by $x_d = +0.8$ mm after a propagation distance of $z = 7$ mm. Note that in the absence of nonlinearity, the displacements of these two beams would have been only ± 0.26 mm. With the minus sign corresponding to beam a it (a , the signal) is displaced by 1.06 mm compared to its original displacement because of two-wave mixing, and beam b (the pump) is displaced by 0.54 mm compared to its original displacement. The spatial “superluminal” behavior occurring outside the original angular sector of propagation is obvious. Overall, Fig. 5 displays good agreement between theory and experiment, although the experimental displacement is somewhat higher.

In conclusion, we have reported the first experimental observation of optical spatial shock waves. These shock waves consist of two kink-type wave fronts, which propagate locked to one another through photorefractive two-wave mixing. We observed that these coupled shock-wave

pairs move undistorted at angles that fall outside their original angular sector of propagation, in a way analogous to that occurring in subliminal/tachyonic temporal Raman shock-wave propagation. Keeping in mind the richness of nonlinear wave phenomena observed in photorefractive materials, the next challenge is to observe shock-wave solitons, that is, very steep kink-antikink wave fronts that do not broaden during propagation.

This work was supported by the DIP German-Israeli Project, by the Israeli Science Foundation, and is also part of the MURI program on optical solitons.

-
- [1] M. A. Meyers, L. E. Murr, and K. P. Staudhammer, *Shock-Wave and High-Strain-Rate Phenomena in Materials* (Marcel Dekker, New York, 1992).
 - [2] M. A. Liberman and A. L. Velikovich, *Physics of Shock Waves in Gases and Plasmas* (Springer-Verlag, Heidelberg, 1986); A. Hasegawa, *Space Plasma Physics* (Springer-Verlag, Berlin, 1989).
 - [3] F.V. Shugaev and L. S. Shtemenko, *Propagation and Reflection of Shock Waves* (World Scientific, Singapore, 1998).
 - [4] Yu. S. Kivshar, Phys. Rev. A **42**, 1757 (1990).
 - [5] D. N. Christodoulides, Opt. Commun. **86**, 431 (1991).
 - [6] G. P. Agrawal and C. Headley III, Phys. Rev. A **46**, 1573 (1992).
 - [7] Yu. S. Kivshar and B. A. Malomed, Opt. Lett. **18**, 485 (1993).
 - [8] D. N. Christodoulides and M. I. Carvalho, Opt. Lett. **19**, 251 (1994).
 - [9] D. Cai *et al.*, Phys. Rev. Lett. **78**, 223 (1997).
 - [10] Self-steepening shocks can also develop in dispersionless nonlinear systems, but no kink solutions are possible. Instead, a wave develops a steep front during propagation. See, for example, F. De Martini *et al.*, Phys. Rev. **164**, 312 (1967); D. Anderson and M. Lisak, Phys. Rev. A **27**, 1393 (1983).
 - [11] M. Haelterman and A. P. Sheppard, Phys. Rev. E **49**, 3389 (1994).
 - [12] S. Pitois, G. Milliot, and S. Wabnitz, Phys. Rev. Lett. **81**, 1409 (1998).
 - [13] S. Darmanyan, A. Kamchatnov, and F. Lederer, Phys. Rev. E **58**, R4120 (1998).
 - [14] A. Kobayakov *et al.*, J. Opt. Soc. Am. B **16**, 1737 (1999).
 - [15] M. I. Carvalho, A. G. Grandpierre, D. N. Christodoulides, and M. Segev, Phys. Rev. E **62**, 8657 (2000).
 - [16] V. A. Vysloukh *et al.*, JETP **84**, 388 (1997).
 - [17] The propagation of optical shock waves is different than shock waves in fluids because here the coupled equations conserve power, whereas in fluids shock fronts are smoothed by dissipation.
 - [18] P. Gunter and J. P. Huignard, *Photorefractive Materials and Their Applications I*, Topics in Applied Physics Vol. 61 (Springer, Heidelberg, 1998).
 - [19] P. Yeh, *Introduction to Photorefractive Nonlinear Optics* (Wiley, New York, 1993).
 - [20] Y. Aharonov, B. Reznik, and A. Stern, Phys. Rev. Lett. **81**, 2190 (1998).